



Synthesis, Characterization and Thermal Studies of Composite Nanofluids and their Comparison with Hybrid Nanofluids

GANESH VEERARAGHAVAN^{1b} and MATHUR RAJESH^{*1b}

Department of Chemical Engineering, SRM Institute of Science and Technology, Kattankulathur-603203, India

*Corresponding author: E-mail: rajeshm@srmist.edu.in; mprajesh@gmail.com

Received: 1 November 2023;

Accepted: 16 February 2024;

Published online: 30 April 2024;

AJC-21604

Ternary nanofluids can either be an admixture of three distinct nanoparticles or the dispersion of a ternary nanocomposite in a base fluid. This work focuses on the synthesis, morphological characterization, stability analysis, estimation and optimization of thermophysical parameters of ternary nanofluids consisting of multiwalled carbon nanotubes, graphene oxide and silver (CNT-GO-Ag). Two cases are considered and compared *viz.* (i) hybrid nanofluids (HNF) prepared from monofluids and (ii) composite nanofluids (CNF) prepared by the dispersion of ternary nanocomposites. The CNF was found to have an enhanced thermal conductivity ratio (k_{nt}/k_b) of 40% as compared to 30% for HNF at 30 °C. This enhancement for the CNF and HNF were found to be 45% and 32%, respectively at the electronic cooling exposure temperature of ~40 to 50 °C. The zeta potential analysis also proved that CNF had superior suspension stability than HNF. The viscosity of CNF was found to be 8% (at 20 °C) to 20% (at 80 °C) lower than HNF, much desired for fluid flow characteristics. Overall, the results show that CNF as compared to HNF possesses superior thermophysical properties with good potential for application in electronic cooling studies.

Keywords: Nanocomposites, Nanofluids, Stability, Thermal conductivity, Viscosity.

INTRODUCTION

Nanofluids, consisting of base fluid(s) and dispersed nanoparticle(s)/nanocomposites, have gained significant warrant in recent years due to their enhanced thermophysical properties. This, in particular, helps widen their potential applications in various processes and industries. Nanofluids are stable suspensions of particles of single species or multiple species but of size range 10-100 nm in base fluid(s). They warrant wide applications due to the combination of solution properties of fluids and nano-sized particles, particularly in heat transfer. Nanofluids can be mono, involving a single species of nanoparticle, or they can be hybrid, involving two or more species. Nanofluids with two different species of nanoparticles are known as binary nanofluids and those with three different species are known as ternary nanofluids [1,2]. The synthesis of nanofluids involves dispersion of nanoparticles or nanocomposites in the base fluid and can be broadly classified in two ways *i.e.* the two-step method and the one-step method.

The two-step method of synthesis is conventional and involves the direct dispersal of nanoparticles in the base fluid. This method facilitates the facile synthesis of nanofluids and is optimal to carry out bulk synthesis (commercial production of nanoparticles) [3]. Furthermore, since the nanoparticles involved are properly purified before addition, there is significantly less chance of impurities and additional compounds being present in the fluid. The process of dispersing the nanoparticles in base fluid is critical and for this, chemical techniques (electrostatic, steric or electrosteric) can be used to maintain and improve the dispersion. One major disadvantage of the method is the agglomeration of nanofluids that happens due to the attractive forces between molecules. This impedes the Brownian motion of dispersed particles which is crucial for many properties, especially, their thermal behaviour. To avoid this, mechanical forces must be used during the entire preparation process or in periodic intervals.

The one-step method is the *in situ* synthesis of nanofluids, involving the reduction of precursors within the fluid medium

itself. Though this produces much more stable nanofluids, its purity is significantly compromised. There are many ways to synthesize nanofluids by the one-step method, apart from the traditional chemical synthesis [4]. Physical vapour condensation, microwave radiation, laser ablation in liquid and ultrasonic-assisted submerged arc are some of the most well-known single-step techniques [5].

The focus is on the application of these fluids in heat transfer studies in microchannels to address electronic cooling. This work deals with the synthesis, characterization and thermal studies of ternary nanofluids of two types *viz.* (i) hybrid nanofluids (HNF) prepared from monofluids and (ii) composite nanofluids (CNF) prepared by the dispersion of ternary nanocomposites.

EXPERIMENTAL

All the chemicals and solvents were procured from Sigma-Aldrich unless mentioned otherwise. All the solutions were prepared in deionized water.

Synthesis of silver nanoparticles: The synthesis process involves reduction of the precursor AgNO_3 by using NaBH_4 as reducing agent. The low temperature was necessitated to prevent the escaping of hydrogen gas [6]. A 300 mL of AgNO_3 solution from the prepared 1 mM stock solution was added dropwise while stirring. A yellow colouration of the solution occurred within 30 s of the reduction, which indicated the formation of silver nanoparticles. The presence of silver nanoparticles was confirmed using LSPR spectrum. The solution was centrifuged for 30 min and subjected to controlled environment drying to obtain the silver powder, which was further characterized for its particle size.

Synthesis of graphene oxide nanopowder: The procured graphite was utilized for the synthesis of graphene oxide through the modified Hummer's method [7,8]. Finally, 3 g of graphene oxide nanopowder was obtained and will be used for hybrid nanofluids.

Preparation of functionalized CNT: Around 3.5 g of MWCNT was functionalized in a 250 mL solution containing H_2SO_4 and HNO_3 (3:1) as described in the literature [9]. The prepared samples were centrifuged at 10000 rpm for about 10-15 min followed by careful decantation of the upper layer. The precipitated powder deposits were scraped out, stored and then dried for a day in oven at 60 °C.

The individual nanoparticles synthesized were dispersed in deionized water in the desired ratio to form various concentrations of nanocomponent by volume fraction (ϕ) as defined in eqn. 1 [1] and sonicated for 240 min. Five different desired concentrations of 0.005, 0.01, 0.015, 0.02 and 0.03 volume fraction (by nanoparticle) were prepared, to form a stable suspension with continuous ultrasonic vibration for 4 h. This probe-sonicated solution was treated as hybrid nanofluid (HNF) and then characterized.

$$\phi = \frac{\sum_{i=1}^3 \left(\frac{m}{p}\right)_{\text{np}i}}{\sum_{i=1}^3 \left(\frac{m}{p}\right)_{\text{np}i} + \left(\frac{m}{p}\right)_{\text{water}}} \quad (1)$$

Preparation of CNT-GO-Ag ternary nanocomposite:

The nanocomposites were prepared using hydrothermal method

based on a modified procedure [1,10]. Functionalized CNT (800 mg) was mixed with GO (800 mg) in 500 mL of 50% ethanol. This was stirred for 60 min and sonicated for 4 h (in two sequences of 30 min stirring and 2 h sonication), the sonicated mixture was tested for nil sedimentation. Then, 200 mL of 0.4 M AgNO_3 was added dropwise into the mixture and then stirred continuously for approximately 2 h to obtain a uniform solution. The solution was agitated once again and combined with 20 mL of 5 mM NaBH_4 solution, which was then heated to 40 °C. The resultant solution was again stirred for another 60 min and sonicated for 2 h. The resultant mixture was centrifuged and subjected to controlled environment drying at 80 °C to obtain CNT-GO-Ag ternary nanocomposite.

RESULTS AND DISCUSSION

Nanofluid characterization

XRD studies: The X-ray diffraction (XRD) was used to analyze the extent of crystalline nature of the prepared samples. Characteristic peaks for Ag (~38°) and carbon were obtained for the CNF sample (Fig. 1). The results suggest amorphous nature of the composite [11,12].

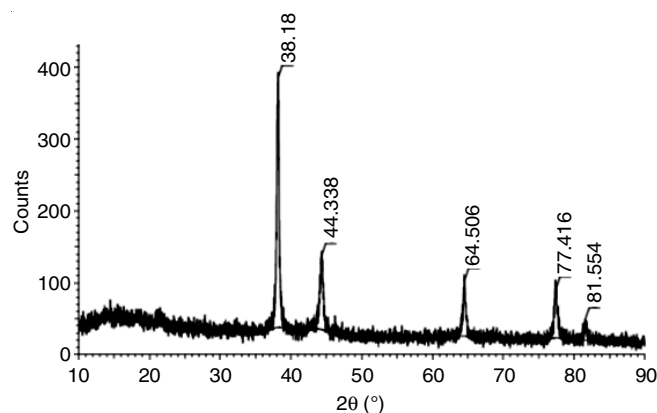


Fig. 1. XRD spectrum of the composite nanofluids

SEM studies: The surface morphology of the synthesized nanocomposite was subjected to microscopic study using a high resolution scanning electron microscope (HRSEM) Thermo-Scientific Apreo S instrument. The magnified images of the CNF (Fig. 2) indicated the layers of plate/sheet exfoliated GO with spherical silver nanoparticles that were embedded on the multi-walled CNTs. The SEM analysis of HNF (Fig. 3) revealed the significant silver agglomeration, suggesting the necessity for more sonication. Along with SEM, EDS analysis revealed prominent peaks corresponding to the presence of oxygen, carbon and silver.

TEM studies: The TEM analysis was done using High-resolution transmission electron microscope (HRTEM), JEOL Japan, JEM-2100 Plus model. The formation of a CNT-GO-Ag nanocomposite was confirmed by the distinct appearance of a unique combination of spherical silver nanoparticles and interwoven plates of GO on the cylindrical rod-shaped multi-walled CNT (Fig. 4). The transmission microscope analysis confirm the sizes of the silver particles in the range of 30 nm.

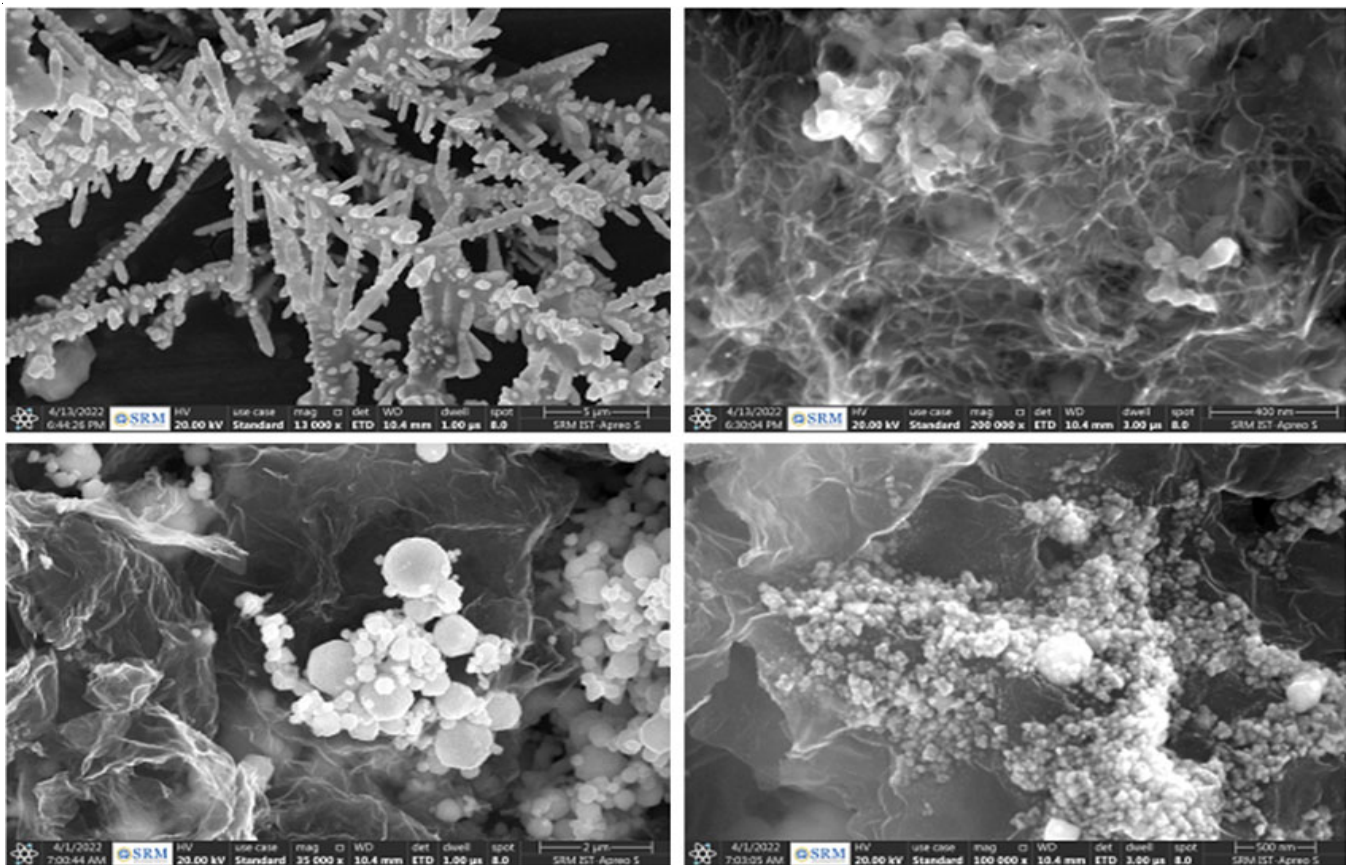


Fig. 2. SEM images of the CNT-GO-Ag nanocomposite

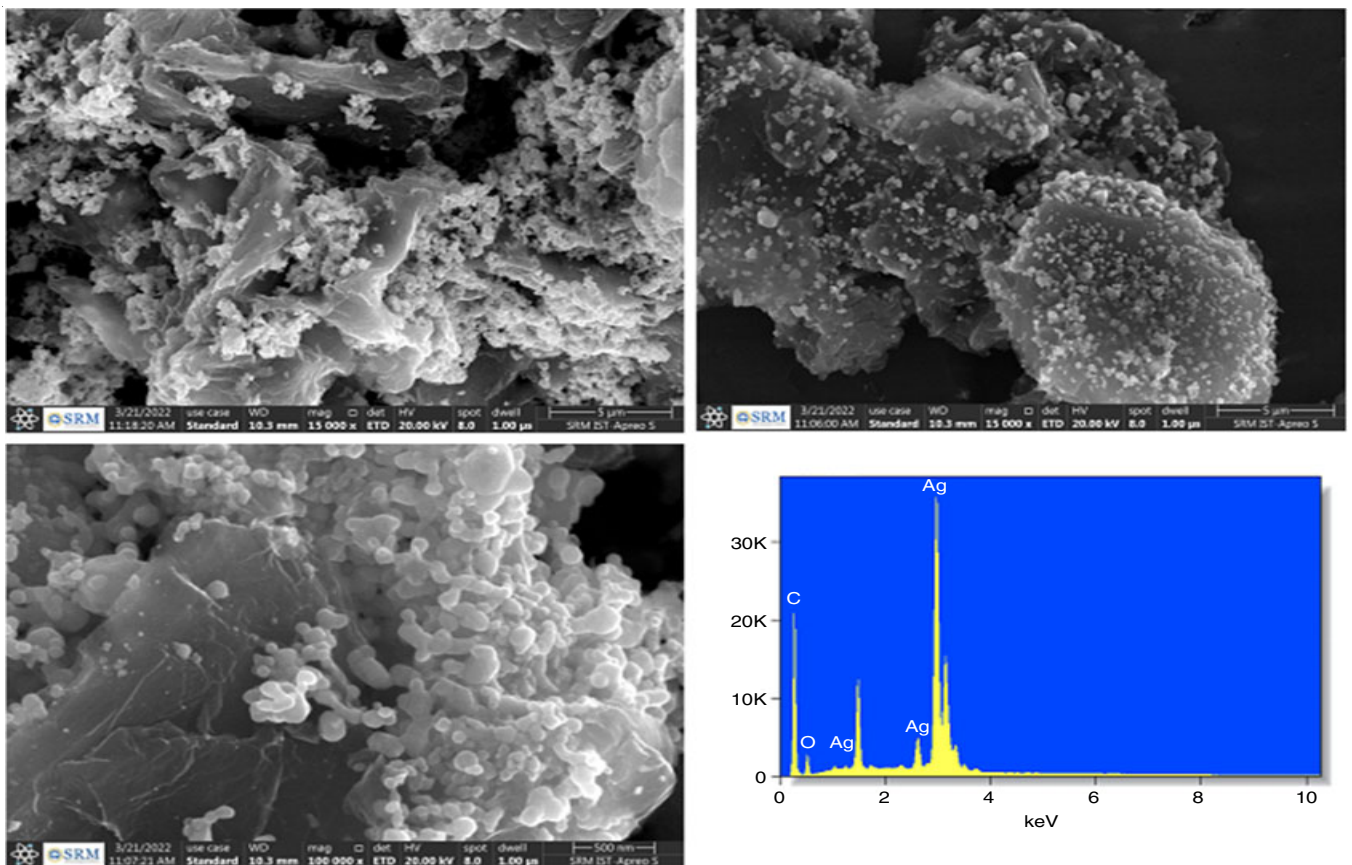


Fig. 3. SEM images of the hybrid nanofluid

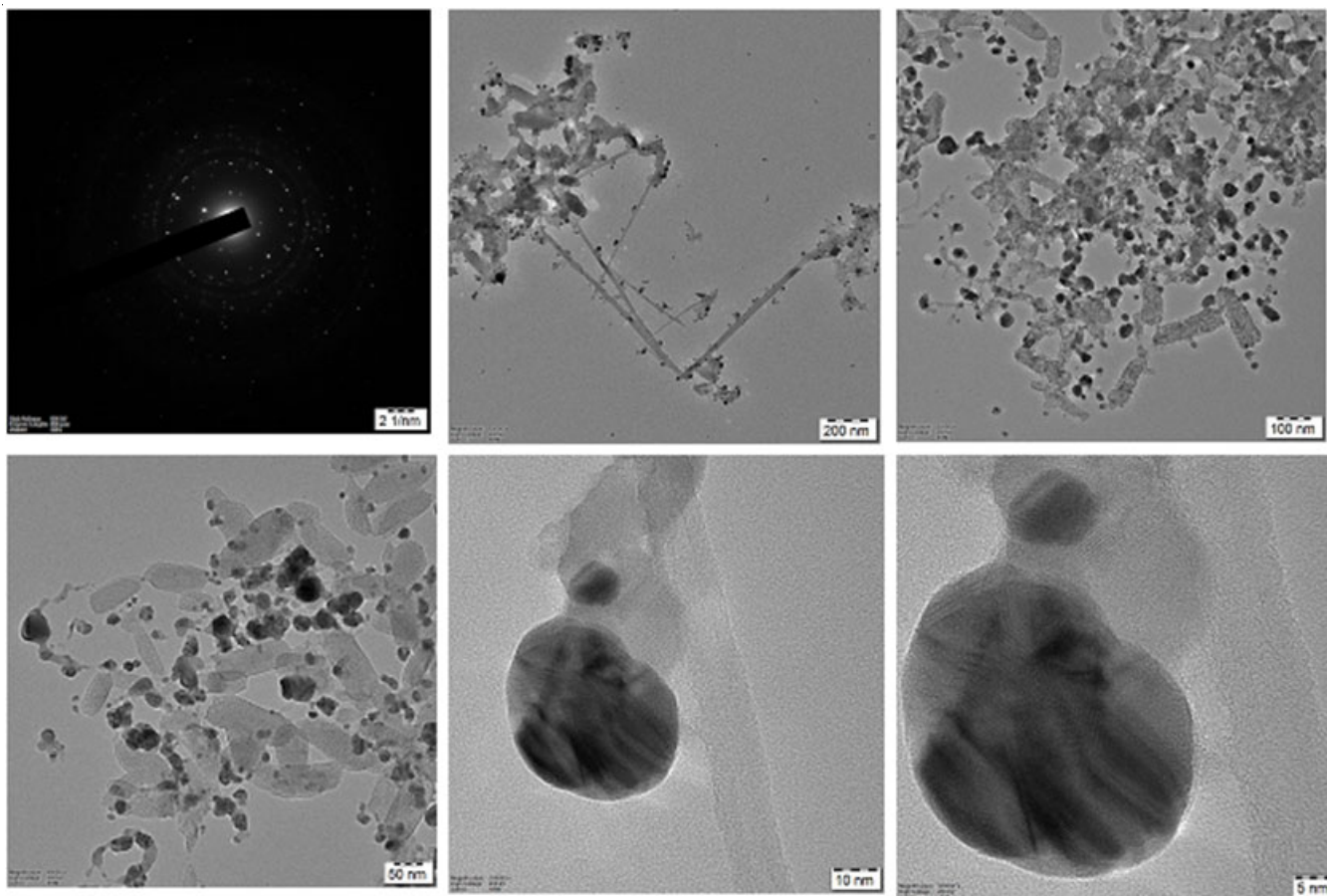


Fig. 4. TEM images of the CNT-GO-Ag nanocomposite

The TEM analysis of HNF (Fig. 5) showed similar composition but with Ag nanoparticles of a relatively bigger size.

Stability of composite nanofluid (CNF): The stability and size analysis of the CNT-GO-Ag nanocomposite dispersion were done using Malvern/Nano ZS-90 Zeta sizer. The stability of the synthesized particles was analyzed for up to 45 days by measuring the zeta potential. Moreover, the Z-average size of nanocomposite was found to be 61.8 nm. The stability of these particles was excellent, as indicated by 62.3 mV zeta potential (Fig. 6).

Hybrid nanofluid (HNF): As for hybrid nanofluid (HNF), the average size of the particles was in the range of 58 nm. The zeta potential -30.3 mV was in the border range of good stability (Fig. 7). Hence, methods to ensure better stability, such as increased ultrasonication and the addition of possible surfactants can be considered, provided the other thermal properties are not compromised. It is to be observed that similar agglomerations were also inferred from the SEM analysis of HNF.

Comparative properties of CNF and HNF: This work specifically focuses on determining and comparing the thermo-

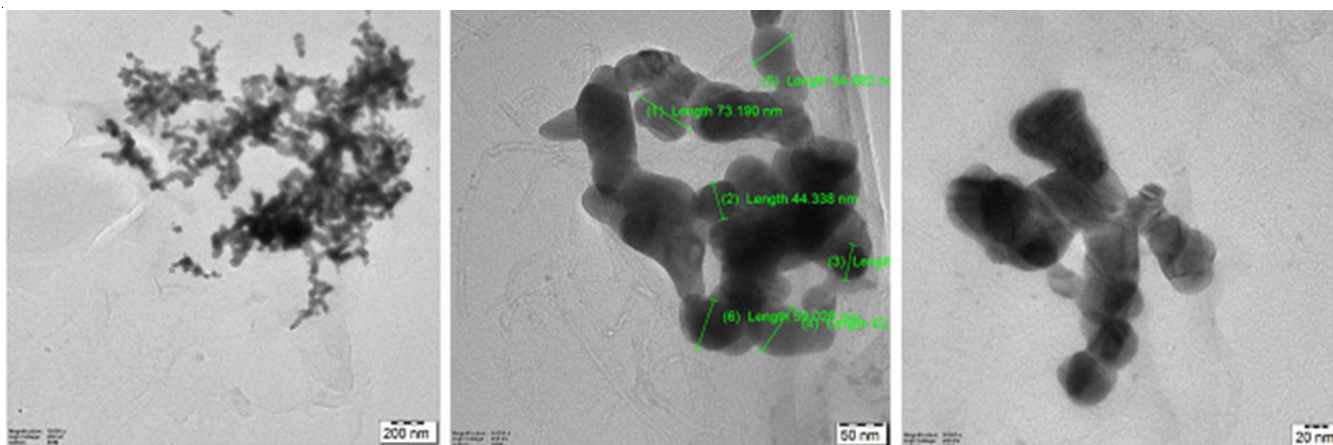


Fig. 5. TEM images of the hybrid nanofluid

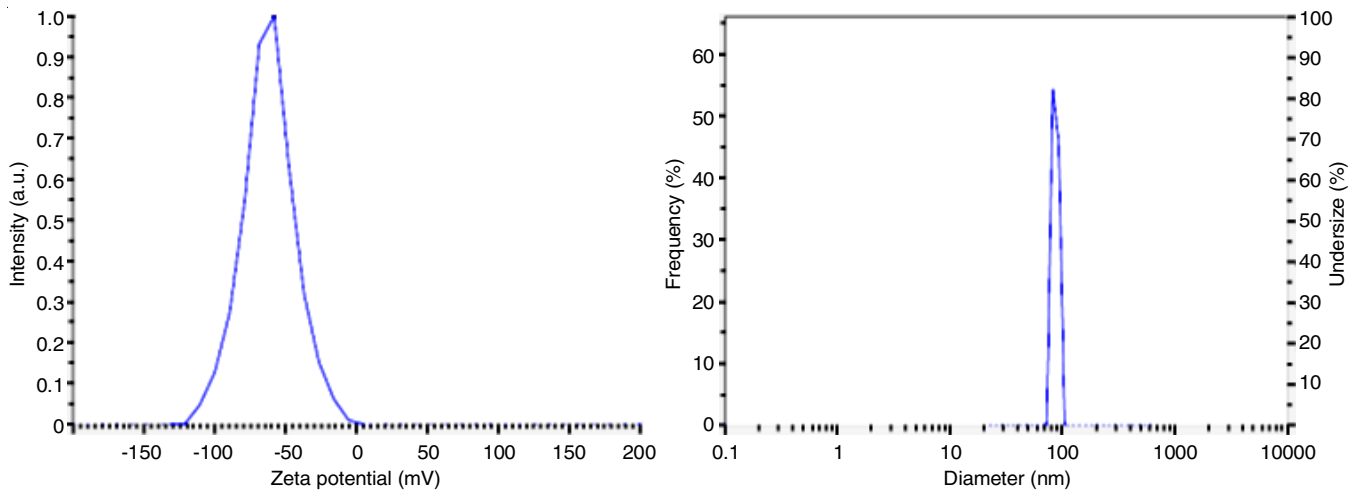


Fig. 6. Zeta potential and size analysis of CNF

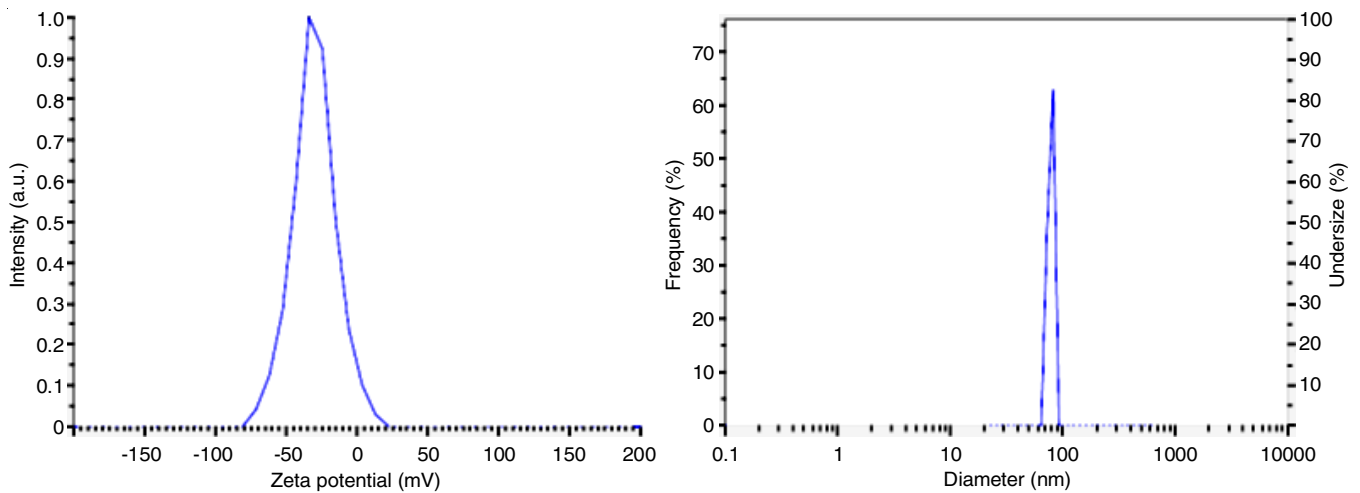


Fig. 7. Zeta potential and size analysis of HNF

physical properties of nanofluids. In accordance, the thermal conductivity, viscosity, density and specific heat capacity of the prepared CNF and HNF were measured over the temperature range of 20-80 °C. The measured values are tabulated in Table-1.

TABLE-1
THERMO-PHYSICAL PROPERTIES OF SYNTHESIZED 3% COMPOSITE NANOFLUIDS AT DIFFERENT TEMPERATURES

Nanofluid	Temp. (°C)	Thermal conductivity (W/m.K)	Viscosity (cP)	Density (g/cc)	Sp. heat capacity (J/g.K)
CNT-GO-Ag	20	0.8389	1.0871	1.0187	3.9878
	30	0.8672	0.8625	1.0183	3.9681
	40	0.8922	0.7079	1.0167	3.9650
	50	0.9125	0.5923	1.0124	3.9812
	60	0.9336	0.5038	1.0094	3.9945
	70	0.9522	0.4370	1.0021	4.0054
	80	0.9674	0.3907	0.9985	4.0180

The thermal conductivity was measured using the Research standard KD2 Pro thermal analyzer (Decagon Devices Inc., USA). This consists of a sensor specifically designed to measure

thermal resistivity of liquid samples at various temperatures and works on the transient hot-wire principle. Various correlations to evaluate the thermal conductivity of mixtures are available in the literature. Among these, the Hamilton-Crosser model (eqn. 2), which is an improvement on Maxwell model, is the most used among researchers working on nanofluids [10]. The significance of this model is its universal application with the significant considerations of very dilute suspension of particles and the ratio $k_{np}/k_b \gg 100$.

$$k_{nf} = \frac{k_{np} + (n-1)k_b + (n-1)(k_{np} - k_b)\phi}{k_p + (n-1)k_b - (k_{np} - k_b)\phi} \cdot k_b \quad (2)$$

where $n = 3/\text{particle sphericity}$; $\phi = \text{volume fraction of the particles}$; k_b and $k_{np} = \text{thermal conductivity of the base fluid and nanoparticle}$.

The measured thermal conductivityES of CNF and HNF are given in Fig. 8, wherein it can be inferred that CNF possesses significantly higher thermal conductivity than HNF across the temperature range, with a maximum value of 0.9674 W/(m.K) observed at 80 °C. This enhancement in thermal conductivity is more emphatically observed in the thermal conductivity ratio, TCR (ratio of thermal conductivity of nanofluid to the thermal

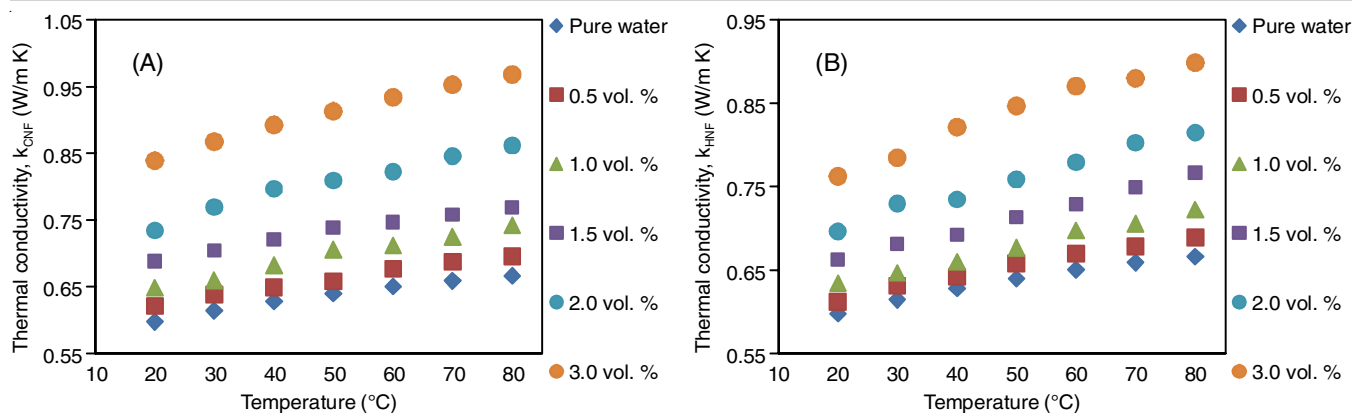


Fig. 8. Variation in thermal conductivity (measured) with temperature for CNF (panel A) vs. HNF (panel B)

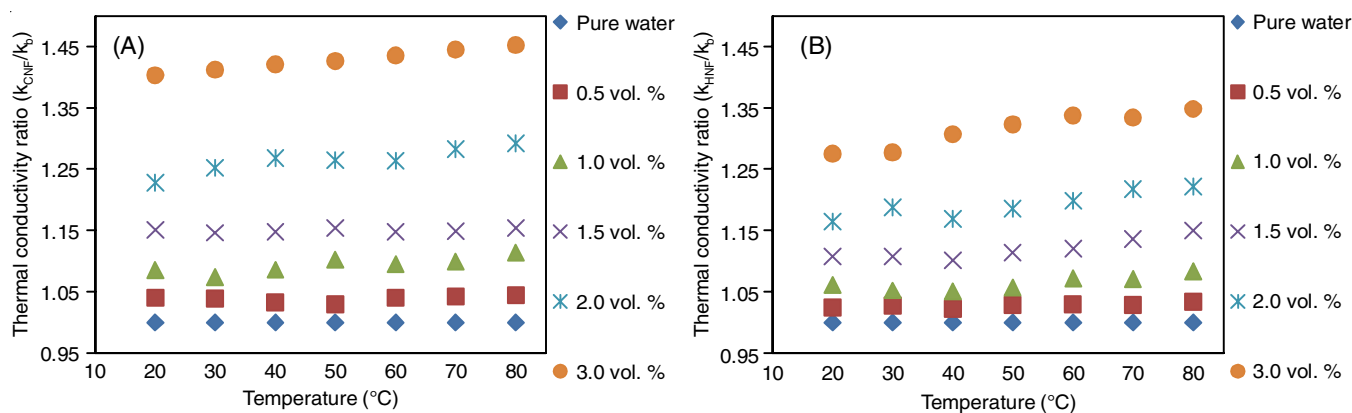


Fig. 9. Variation in thermal conductivity ratios (measured) with temperature for CNF (panel A) vs. HNF (panel B)

conductivity of base fluid measured at the same temperature) variation with temperature (Fig. 9). The TCR peaks at around 1.45 and 1.35 at 80 °C for CNF and HNF, respectively. The measured thermal conductivity of CNF and HNF were compared with the correlation and the obtained values were significantly higher, especially at the higher temperatures (Fig. 10).

Viscosity: Brookfield viscometer was used for estimating viscosity for various volume fractions. The measured viscosity values were then compared with the well-known Brinkman model [10,13] given by eqn. 3:

$$\mu_{nf} = (1 + 2.5\phi)\mu_b \quad (3)$$

where μ_{nf} = exhibited viscosity of the nanofluid and μ_b = viscosity of the base fluid.

The viscosity of CNF does increase with concentration of nanocomposites as shown in Fig. 11. It is deduced that CNF exhibits a very small percentage variation from the correlation (less than 1%, with the exception of 80 °C, where it is 2.5%), but HNF exhibits significantly larger deviations (maximum of 5.5%) (Fig. 11). Viscosity being one of the core fluid properties for heat transfer applications, the CNF being less viscous holds higher advantage over the HNF across the temperature range.

Density: Anton Paar density meter was used for measuring the density of the nanofluids. The density thus quantified is finally compared with the established Pak & Cho [10] correlation as given in eqn. 4:

$$\rho_{nf} = (1 - \phi)\rho_b + \phi\rho_{np} \quad (4)$$

where ρ_{nf} is the effective density of the nanofluid. ρ_{np} and ρ_b are the weighted densities of particles and base fluids respectively. The density variation of CNF of various dilutions increases with composition, as expected, due to the higher density of the particles, but decreases with temperature due to their base fluid behaviour (Fig. 12b).

Specific heat capacity: The specific heat capacity, being one of the vital thermal properties of the fluids, especially in convective mode, was measured using a differential scanning calorimeter (DSC), NETZSCH, Germany. The obtained values are compared with the following correlation [10]:

$$\rho c_{p,nf} = (1 - \phi)\rho_b \cdot c_{p,b} + \phi\rho_p \cdot c_{p,p} \quad (5)$$

where $c_{p,nf}$ is the overall specific heat capacity of nanofluid, $c_{p,p}$ and $c_{p,b}$ are the specific heat capacity of the nanoparticles and base fluid, respectively. As for the specific heat capacity of CNF, it decreases with increasing concentration (Fig. 12a), whereas the deviation from correlation is slightly less for CNF compared to HNF (Fig. 11).

Since the overall work involves the usage of these nanofluids in microchannel heat transfer, the thermal conductivity is given additional treatment. Based on the results, the best fit obtained for the thermal conductivity, $k_{cnf}(f(x,y))$ as a function of volume %, $\phi(x)$ and temperature, $T(y)$ is given below:

$$f(x,y) = a_{00} + a_{10}x + a_{01}y + a_{20}x^2 + a_{11}xy$$

where the estimated coefficients based on the 95% CL are: $a_{00} = 0.5607$; $a_{10} = 0.0334$; $a_{01} = 0.0019$; $a_{20} = -0.0141$; $a_{11} = 0.0003$.

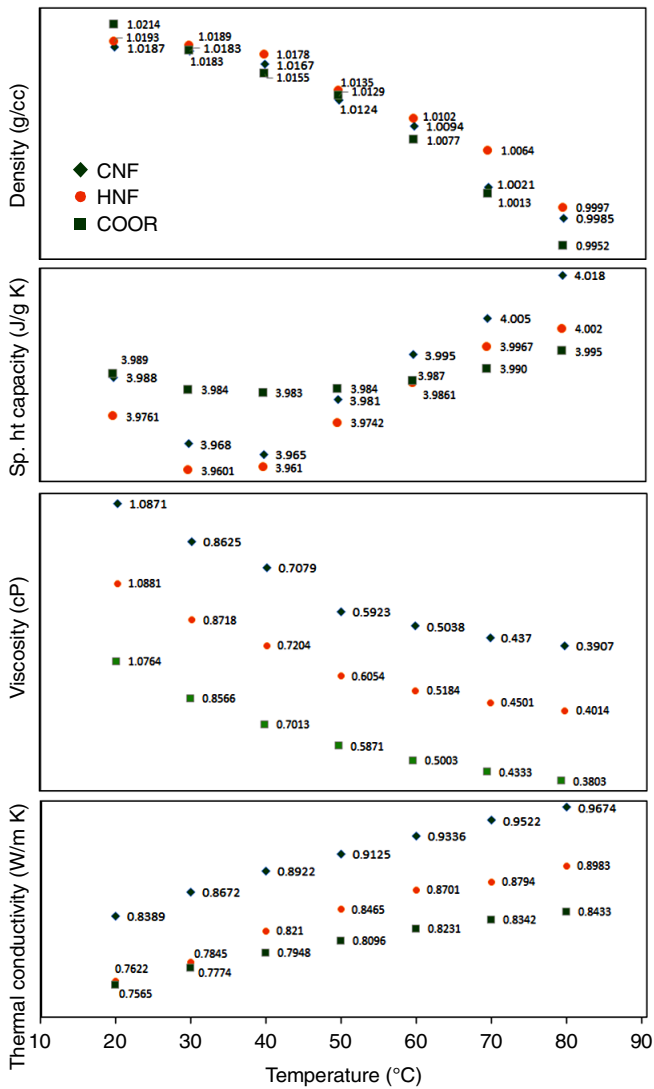


Fig. 10. Overview of thermophysical properties of 3% CNF and HNF (measured and correlation), at various temperatures

Extended to the real variables:

$$k_{cnf}(\phi, T) = 0.5607 + 0.0334\phi + 0.0019 T - 0.0141\phi^2 + 0.0003 T\phi$$

The surface plot and the parity plot for the data fitness are given in Figs. 13 and 14, respectively.

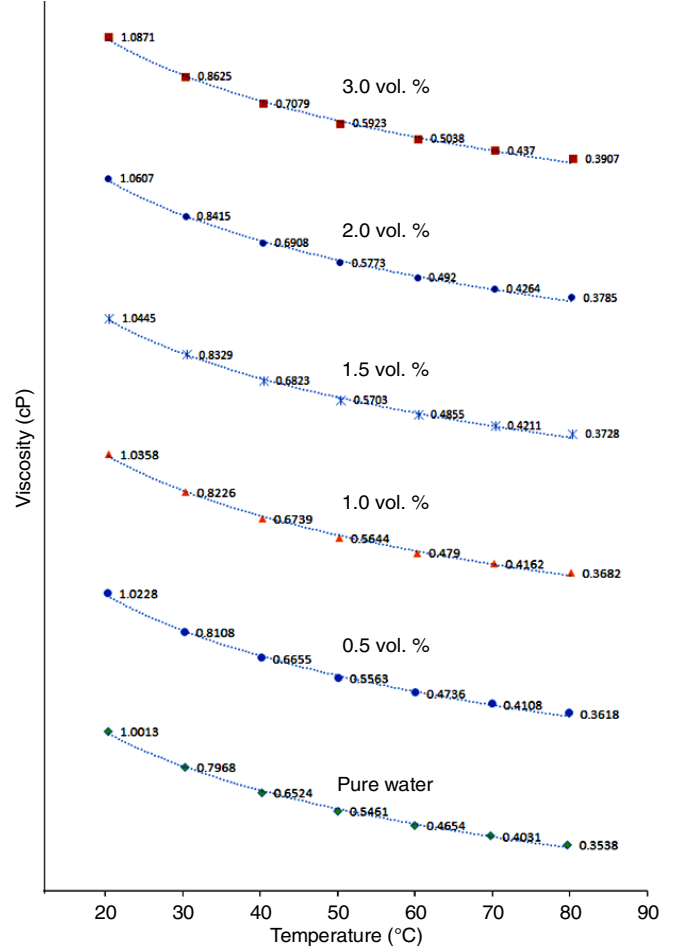
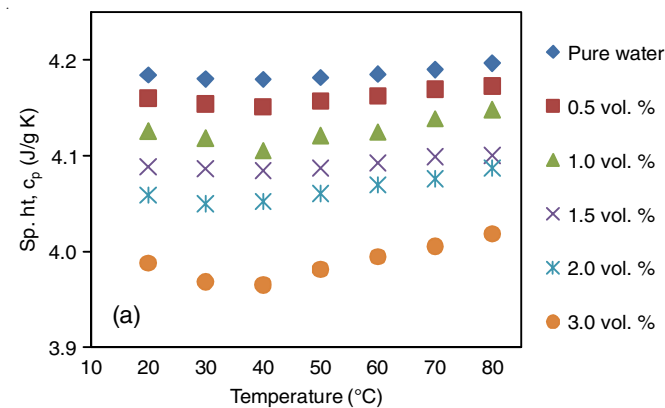


Fig. 11. Measured viscosity of CNF vs. temperature

Conclusion

This work involves the synthesis and characterization of ternary hybrid nanofluid and tri-species composite nanofluid. It is envisaged as the primary step for heat transfer studies in microchannels to address the broader study of electronic cooling. This study attempts to address the qualitative and quantitative differences between hybrid nanofluids (HNF) containing nanoparticles and composite nanofluids (CNF) containing nanocomposites. The morphological analysis of two nanofluids gave similar results, whereas the stability of CNF was of an

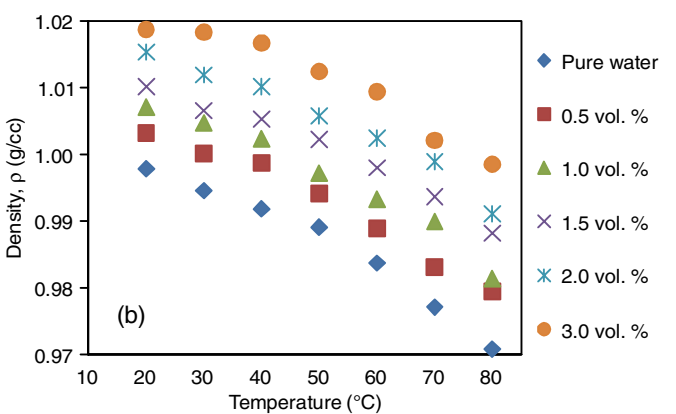
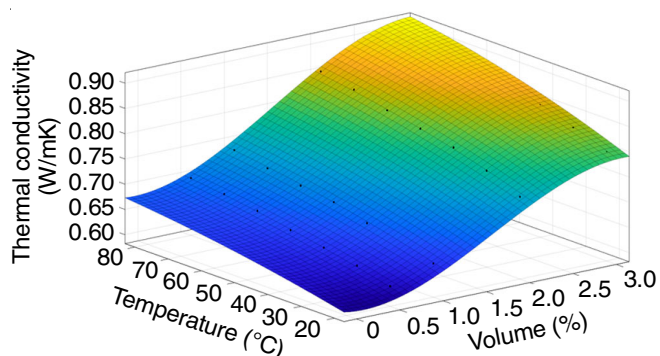
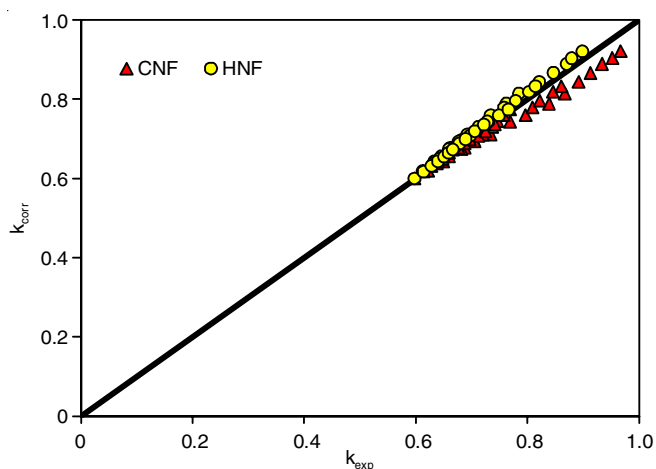


Fig. 12. (a) Measured Sp. ht capacity of CNF vs. temperature; (b) Measured density of CNF vs. temperature

Fig. 13. Surface plot for k_{cnf} vs. temp (T) vs. vol %Fig. 14. Parity plot for $k_{\text{experimental}}$ vs. $k_{\text{correlation}}$

enhanced nature than the HNF. The CNF was found to possess enhanced thermal conductivity ratio (k_{nf}/k_b) by 40% compared to 30% for the HNF at 30 °C, whereas the same was 45% and 32% at the more practical exposure temperature (electronic cooling) of 40-50 °C. Also, the viscosity of CNF is less than that of HNF by 8% to 20%. This plays a vital role in the flow across the channels and has a significant role in the associated pressure drops. With these significant desired properties, namely, increased thermal conductivity, increased stability and decreased viscosity of CNF than that of HNF, the authors intend to proceed with the CNF for the desired application due to the potential advantages mentioned and also due to the absence of any tendency that poses a potential pulldown of the intended performance.

ACKNOWLEDGEMENTS

The authors acknowledge SRM Central Instrumentation Facility (SCIF), SRMIST for providing the instrumentation facilities.

CONFLICT OF INTEREST

The authors declare that there is no conflict of interests regarding the publication of this article.

REFERENCES

- J.M. Zayan, A.K. Rasheed, A. John, W.F. Faris, A. Aabid, M. Baig and B. Alallam, *Materials*, **16**, 173 (2022); <https://doi.org/10.3390/ma16010173>
- J. Sarkar, P. Ghosh and A. Adil, *Renew. Sustain. Energy Rev.*, **43**, 164 (2015); <https://doi.org/10.1016/j.rser.2014.11.023>
- Z. Haddad, C. Abid, H.F. Oztop and A. Mataoui, *Int. J. Therm. Sci.*, **76**, 168 (2014); <https://doi.org/10.1016/j.ijthermalsci.2013.08.010>
- J.A. Ranga Babu, K.K. Kumar and S. Srinivasa Rao, *Renew. Sustain. Energy Rev.*, **77**, 551 (2017); <https://doi.org/10.1016/j.rser.2017.04.040>
- K.Y. Leong, K.Z. Ku Ahmad, H.C. Ong, M.J. Ghazali and A. Baharum, *Renew. Sustain. Energy Rev.*, **75**, 868 (2017); <https://doi.org/10.1016/j.rser.2016.11.068>
- X.F. Zhang, Z.G. Liu, W. Shen and S. Gurunathan, *Int. J. Mol. Sci.*, **17**, 1534 (2016); <https://doi.org/10.3390/ijms17091534>
- H. Yu, B. Zhang, C. Bulin, R. Li and R. Xing, *Sci. Rep.*, **6**, 36143 (2016); <https://doi.org/10.1038/srep36143>
- Y. Zhu, S. Murali, W. Cai, X. Li, J.W. Suk, J.R. Potts and R.S. Ruoff, *Adv. Mater.*, **22**, 3906 (2010); <https://doi.org/10.1002/adma.201001068>
- C. Jin, Q. Wu, G. Yang, H. Zhang and Y. Zhong, *Powder Technol.*, **389**, 1 (2021); <https://doi.org/10.1016/j.powtec.2021.05.007>
- B.C. Pak and Y.I. Cho, *Exp. Heat Transf.*, **11**, 151 (1998); [https://doi.org/10.1016/S0017-9310\(99\)00369-5](https://doi.org/10.1016/S0017-9310(99)00369-5)
- A. Khan, A.A.P. Khan, A.M. Asiri and B.M. Abu-Zied, *Compos., Part B Eng.*, **86**, 27 (2016); <https://doi.org/10.1016/j.compositesb.2015.09.018>
- J.D. Kim, H. Yun, G.C. Kim, C.W. Lee and H.C. Choi, *Appl. Surf. Sci.*, **283**, 227 (2013); <https://doi.org/10.1016/j.apsusc.2013.06.086>
- L.S. Sundar, K.V. Sharma, M.T. Naik and M.K. Singh, *Renew. Sustain. Energy Rev.*, **25**, 670 (2013); <https://doi.org/10.1016/j.rser.2013.04.003>